

Experimental Determination of the Translational Acceleration Values for a Spinning Vehicle

Oren Masory, Erwan Le Gall
Florida Atlantic University
Boca Raton, FL
1-561-297-3424
masoryo@fau.edu

Wade Bartlett
Mechanical Forensics
Engineering Services, LLC
Rochester, NH
wade.bartlett@gmail.com

Bill Wright
Traffic Accident Reconstruction Origin
West Palm Beach, FL
bwright@tarorigin.com

ABSTRACT

Accident reconstructionists often determine pre-collision conditions based on post-collision evidence. Energy-based speed calculations for skidding vehicles are commonly used and have been the basis for numerous theoretical and experimental works. The simplest analysis technique, “skid-to-stop” is fairly well understood, however the more complex circumstance of a spinning trajectory is less well understood. This paper will describe a series of experiments conducted to evaluate the frictional values applicable to a spinning vehicle as it rotates and translates without brake application.

Keywords

Spinning, post-impact, rotation, friction

1. INTRODUCTION

Accident reconstruction is the application of scientific principles to motor vehicles collisions in order to determine pre-collision states based on post-collision evidence. These conclusions usually involve speed, direction, and location for all involved vehicles.

One commonly used principle is that of “conservation of energy,” which is actually an application of the First Law of Thermodynamics. In such an analysis, the reconstructionist quantifies the work done by a vehicle as it skids on the road surface and equates it to the kinetic energy possessed by the vehicle at the start of the skid. Once energy is known speed follows directly.

Skid marks, such as shown in Figure 1, are made by a tire that is moving but not free to roll. This circumstance can be simply modeled with relatively accurate results [Reed 1987, Neptune 1995]. To complete such an analysis, one needs only know the skid length and the tire-roadway friction coefficient.

Values for static tire-road friction fall into fairly predictable ranges. In most cases this value is estimated. But when the consequences are large, such as a criminal prosecution, testing is often done to reduce uncertainty and yield more accurate speed estimates.

Figure 2 shows a typical acceleration curve generated during a skid-test. This characteristic curve clearly shows the tires transitioning through the maximum-generated friction (f_{peak})



Figure 1. Typical locked-wheel skid marks.

then settling to the value of kinetic friction as the vehicle skids to rest. Brake balance, vehicle configuration, and application rate will dictate how closely the maximum friction achieved by a vehicle will approach the static friction value for a single tire.

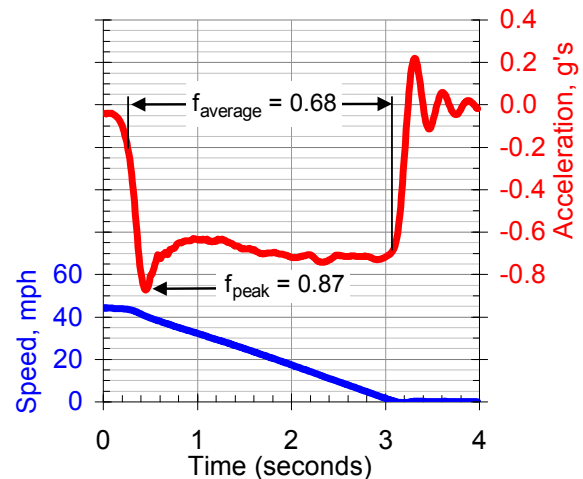


Figure 2. Typical “skid curve” showing acceleration and speed as a function of time during a skid test.

Evaluating an average or effective friction value from such data was discussed by Reed [1988], Robinson [1994], and Goudie [2000]. The average friction is then multiplied by the weight of the vehicle to find the force exerted, and that quantity is multiplied by the distance over which the force was applied to determine the amount of work accomplished.

In ordinary driving, a nearly static relationship exists between the tire contact face and the roadway. This is a near-zero slip condition in both longitudinal and lateral directions. Skidding, on the other hand, represents 100% longitudinal slip, and has been shown to be easy to model and understand in the context of energy analysis. The case of partial longitudinal slip, though, as a result of partial braking or ABS-controlled braking lies somewhere between those two extremes, with peak braking friction generally occurring between 15 and 20% slip.

Slip frequently presents itself in collision evidence. Longitudinal slip is easily distinguished from skid mark evidence, while lateral slip can be associated with a vehicle that is turning or spinning. Such a spin can be caused by overly aggressive steering maneuvers or collision forces. Side-slip occurs when a tire is free to roll, but is moving in a direction that is not parallel with the direction it is pointing. Tire marks made by a vehicle in such a condition are shown in Figure 3, while the forces acting on that vehicle are shown in Figure 4.



Figure 3. Tire marks from a vehicle side-slipping (yawing) while translating.

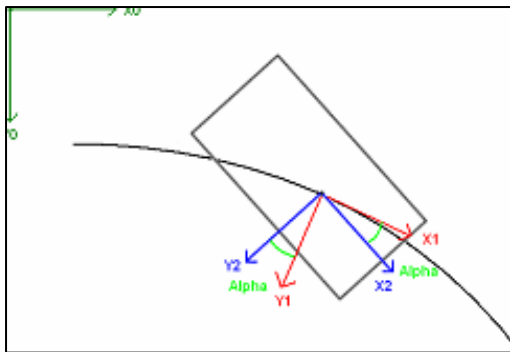


Figure 4. Forces acting on a vehicle which is side-slipping (yawing) while translating.

Side-slip can be thought of as occurring when the vehicle's velocity is not coincident with the direction it is pointing. In Figure 4, the vehicle has an instantaneous velocity in the X1 direction while it is pointing in the X2 direction. The difference between these two directions, α , is called the slip-angle.

In addition to considering the slip-angle of the vehicle, as shown in Figure 4, for overall average effects, one must sometimes also consider the slip angles experienced by individual tires. An unbraked tire traveling at slip angles

between 0 and 90 degrees will be rotated by the component of the roadway frictional force that is perpendicular to the tire's axis of rotation (parallel to the direction the tire is facing). When slip equals 90° there is no component of force to rotate the tire and it stalls, or stops turning. In practice, it has been observed that for slip angles within a few degrees of 90°, the resistance to motion in the wheel and hub components is sufficient to overcome this effect and the wheel stops turning regardless of vehicle velocity.

2. THE MODEL

A free-rolling tire operating at zero slip angle ($\alpha = 0^\circ$) generates only the small forces that are associated with rolling resistance while a free-rolling tire moving laterally ($\alpha = 90^\circ$) does not roll and fits the 100% slip skid-mark model detailed above. Several models have been suggested to quantify tire forces between these extremes as a function of the slip angle. One such simple model was presented by Martinez [1996]:

$$\mu_{Effective} = \mu(\sin(\alpha))$$

In this model, μ is the 100%-slip coefficient of friction determined from skid tests, and alpha is the slip angle of the vehicle. The instantaneous component of tire road friction opposing vehicle velocity, $\mu_{Effective}$, acts to slow the vehicle. While this model is intuitive, no published data existed to verify its accuracy.

3. EXPERIMENTS

3.1 Equipment

A series of full-scale experiments were conducted to verify the model. In these experiments a vehicle was instrumented with a high resolution, fast sampling VBOX-III GPS-based data acquisition system from Racelogic (shown in Figure 5). Vehicle spin was induced through aggressive steering maneuvers on dry pavement.

The system uses a survey grade 100Hz GPS that calculates each measurement 100 times a second without interpolation, so that each reading is independent of all previous readings. Once position is known accurately, distance, velocity, and acceleration can be calculated at each step. The data is stored on a removable compact flash card.

In addition to the main system, the VBOX Inertial Measurement Unit (IMU) was utilized, shown in Figure 6. It houses three $\pm 150^\circ/s$ yaw rate sensors and a tri-axial $\pm 1.7g$ accelerometer pack. The IMU connects directly to the VBOXIII for simultaneous sampling.



Figure 5. Racelogic VBOX-III main unit



Figure 6. VBOX-III IMU from Racelogic.

3.2 Test Procedures

Experiments were conducted on a dry asphalt parking lot at Florida Atlantic University. Two vehicles were tested: a 1992 Oldsmobile Achieva, a front-wheel drive four-door-sedan, and a 2004 Chevrolet Corvette, a rear wheel drive two door sport coupe. Two methods were used to induce spin: a double/triple multiple steer while traveling forward and a “caster-steer” maneuver while moving in reverse, as described below.

Multiple Steer: In a multiple-steer maneuver the initial slip was induced by a quick steering input resulting in an over-steering condition with a modest amount of slip. As the car approached its maximum slip angle, it was steered in the opposite direction resulting in a larger slip angle. A third steering input was sometimes required to achieve the desired rotation rate and subsequent spin. Steering inputs were timed to achieve progressively increasing slip angles.

Caster Steer: In this technique the car was driven in reverse and a brisk steering input was initiated to begin to turn. Positive caster settings aided in obtaining high angular acceleration. Angular rates built quickly and inertial forces overwhelmed available tire forces, initiating spin. This method proved to be simple and highly repeatable.

Skid tests were conducted to determine the baseline μ value. These tests generated a characteristic curve similar to that shown in Figure 2 with $\mu_{Average} = 0.54$, and $\mu_{Peak} = 0.70$.

4. RESULTS

4.1 Experimental Data

Approximately 40 experiments were conducted. Analysis revealed that the accelerations derived solely from the GPS-position data had a secondary sinusoidal signal imposed on the channels of interest, rendering them less useful than the IMU results. It was hypothesized that the undesired artifacts might be a result of VBOX software algorithms. The accelerometer data was significantly cleaner and proved more reliable for the features of interest to this paper.

Analysis required resolving differences between the accelerations recorded with respect to the trajectory-referenced coordinate system (X1), and the vehicle-referenced system (X2). The difference in the orientation of these systems represented the slip angle α shown in Figure 7.

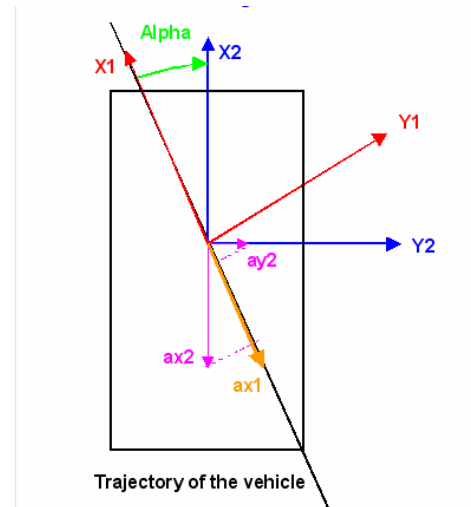


Figure 7. Trajectory based reference system (X1-Y1) and vehicle-based reference system (X2-Y2).

Figure 8 shows a representative $\mu_{Effective}$ versus slip-angle curve generated during a caster-steer maneuver using the Oldsmobile, along with the model presented earlier.

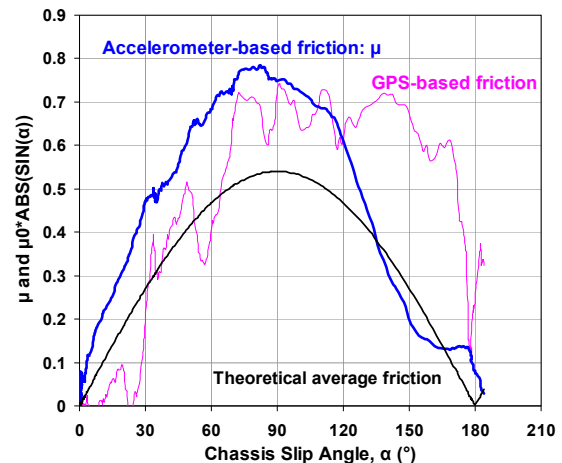


Figure 8. Comparing theoretical and experimental results for $\mu_{Effective}$ as a function of slip angle for one spin test

The friction value measured in several tests showed a plateau or even a noticeable dip at slip angles near 90 degrees, with the friction sometimes dropping as low as the average friction value, as shown in Figure 9, taken from one Corvette test.

4.2 Discussion of Results

The curve in Figures 8 and 9 are seen to be approximately symmetric about 90°, as expected. The measured friction values generally show a positive bias at all slip angles other than near $\alpha=90^\circ$. In this portion of the travel, the tire’s heading direction is perpendicular to its velocity. That is to say that the tire is moving but not free to roll which is exactly how a skidding tire was defined. In this region, $\mu_{Effective}$ tends to decay to the predicted value of $\mu_{Average}$ as a result of the tires’ ceasing to rotate.

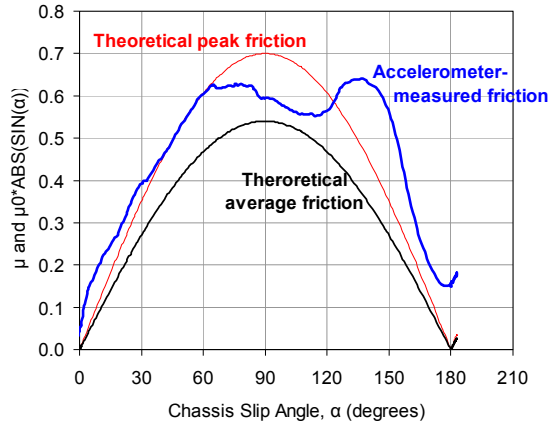


Figure 9. Comparing experimental results for $\mu_{Effective}$ to peak and average theoretical values, showing a dip near mid-rotation where wheels cease to rotate.

The portion of travel when slip angles are between 0 and 90° is analogous to a partially-braked tire with slip somewhere between zero (free-rolling) and 100% (locked and skidding). The relationship between friction and slip-angle is similarly non-linear, but does monotonically increase towards a peak value at some point where it is not yet sliding sideways. Gillespie [1992] and Dixon [1996] showed that the lateral forces reach near-maximum values at relatively low slip angles (12 to 15 degrees). It is hypothesized that the positive friction bias observed in Figures 8 and 9 are a result of the tires' operating at a level proportional to $SIN(\mu_{Peak})$ rather than $SIN(\mu_{Average})$ as had been initially expected. This higher frictional capability was seen to extend only to the point where one or more tires ceased to rotate as they approached 90° side slip.

The curves also generally showed a slight shift to the left as compared to the theoretical predictions. It is hypothesized that this is due to the fact that the steered tires' slip angle is leading the chassis slip angle slightly, as shown in Figure 9. This effect was more prevalent in the Oldsmobile tests because the Oldsmobile carried a much higher percentage of the overall weight on the front wheels, exaggerating this steering-effect.



Figure 9: Front and rear tires are not parallel during steer maneuver (view from rear).

4.3 Future Testing

Several deficiencies were noted in the current round of experiments. The most significant of these was the lack of documentation of steer angles during the slip angle events. Resolving the variation in tire slip angles to allow calculation of the slowing friction at each wheel end will improve the fidelity of the model significantly. Further improvements may be gained by accounting for the weight shift which occurs during such events. Follow up experiments will gather data to correct for this deficiency.

5. CONCLUSION

The translational slowing rate of a vehicle in a state of spin was examined. The simple model presented compared reasonably well with test results, though it was observed that tire forces are more closely related to static friction than kinetic friction for much of the spin event. Additional experiments are suggested to refine the results.

6. REFERENCES

- [1] Dixon, John C., Tires, Suspension and Handling, Dynamics, Society of Automotive Engineers, Warrendale, PA, 1992, ISBN 1-56091-831-4, pg. 96-99
- [2] Gillespie, Thomas D., Fundamentals of Vehicle Dynamics, Society of Automotive Engineers, Warrendale, PA, 1992 ISBN1-56091-199-9, pg. 350-364
- [3] Goudie, D.W., J. J. Bowler, C. A. Brown, B. E. Heinrichs, G. P. Seigmund, Tire friction during locked wheel braking, SAE paper 2000-01-1314
- [4] Martinez, J. E., R. J. Schlueter, A primer on the reconstruction and presentation of rollover accidents, SAE paper 960647
- [5] Neptune, J. A., J. E. Flynn, P. A. Chavez, H. W. Underwood, Speed from skids: A modern approach, SAE Paper 950354
- [6] Reed, W. S., A. T. Keskin, Vehicular response to emergency braking, SAE Paper 870501
- [7] Reed, W. S., A. T. Keskin, A comparison of emergency braking characteristics of passenger cars, SAE Paper 880231
- [8] Robinson, E. L., Analysis of accelerometer data for use in skid-stop calculations, SAE Paper 940918